

## NOTE

## Agrosystems

# A statistical approach to surface renewal: The virtual chamber concept

Bruce B. Hicks<sup>1</sup>  | Nebila Lichiheb<sup>2</sup> | Deb. L. O'Dell<sup>3</sup>  | Joel N. Oetting<sup>3</sup> | Neal S. Eash<sup>3</sup> | Mark Heuer<sup>2</sup> | LaToya Myles<sup>2</sup>

<sup>1</sup> MetCorps, P.O. Box 1510, Norris, TN 37828, USA

<sup>2</sup> National Oceanic and Atmospheric Administration, Atmospheric Turbulence and Diffusion Division, P.O. Box 2456, Oak Ridge, TN 37831-2456, USA

<sup>3</sup> Dep. of Biosystems Engineering and Soil Science, Univ. of Tennessee Institute of Agriculture (UTIA), 2506 E.J. Chapman Drive, Knoxville, TN 37996, USA

## Correspondence

Bruce Hicks, MetCorps, P.O. Box 1510, Norris, TN 37828, USA.  
Email: [hicks.metcorps@gmail.com](mailto:hicks.metcorps@gmail.com)

Assigned to Associate Editor Varaprasad Bandaru.

## Funding information

US National Science Foundation, Grant/Award Numbers: AGS 12-33458, AGS12-36814; The University of Tennessee

## Abstract

In the stable conditions prevailing at night, concentrations of emitted gases (e.g., radon [Rn], carbon dioxide [CO<sub>2</sub>], methane [CH<sub>4</sub>], ammonia [NH<sub>3</sub>], and nitrous oxide [N<sub>2</sub>O]) build up at the surface, with intermittent interruptions due to the passage of packets of turbulence. The applicability of conventional experimental methods is then questionable. Here, a statistical approach is proposed, in which micrometeorological field data are used to replicate the likely characteristics of a chamber experiment, yielding estimates of surface fluxes at the surface itself with reduced requirement for adequate fetch. Application of the virtual chamber methodology to two recent field studies is explored: (a) a study of nocturnal CO<sub>2</sub> emission from a farmland area in Ohio in 2015; and (b) an investigation of NH<sub>3</sub> effluxes from a crop previously treated with urea ammonium nitrate (UAN) in Illinois in 2014. For both datasets, the virtual chamber approach yields results in general agreement with eddy covariance (EC) data.

## 1 | INTRODUCTION

Quantification of the emission rates of trace gases from soils, swamps, etc. often presents a problem that standard micrometeorological methods fail to solve (Skiba et al., 2009; Wilson et al., 2012). While the various eddy-covariance techniques have gained popularity, their requirement for good fetch (especially at night) remains an obstacle that is difficult to overcome (Aubinet, 2008). Bowen ratio methods are less susceptible to fetch limitations, because relevant measurements can

be made at a lower height than for eddy-covariance (EC) or flux/gradient calculations (Meyers et al., 1996).

Measurement of fluxes at night is especially demanding (Darenova et al., 2014; Schneider et al., 2009). To address the matter of emissions from soil at night, field programs often rely on measurement methods of an entirely different kind – the use of chambers that confine emissions from the ground within closely monitored volumes, thus eliminating the problems associated with fetch. In the case of carbon dioxide (CO<sub>2</sub>), for example, the rate of increase in CO<sub>2</sub> concentrations within such a confined volume is an indication of the flux from the surface. However, it is recognized that the presence of any such chamber imposes an obstacle to the natural flow regime, with consequences that are hard to quantify.

**Abbreviations:** BREB, Bowen ratio energy balance; EC, eddy covariance; UAN, urea ammonium nitrate.

This is an open access article under the terms of the [Creative Commons Attribution](https://creativecommons.org/licenses/by/4.0/) License, which permits use, distribution and reproduction in any medium, provided the original work is properly cited.

© 2021 The Authors. *Agrosystems, Geosciences & Environment* published by Wiley Periodicals LLC on behalf of Crop Science Society of America and American Society of Agronomy

Comparisons among results obtained using chambers of different configurations have been revealing. Comparison of results from closed (“static”, q.v. Edwards, 1982) chambers and alternative “dynamic” approaches (Norman et al., 1992) has received particular attention. Field studies summarized by Nay et al., (1994) have indicated considerable differences, sufficient that laboratory tests were conducted, involving the measurement of CO<sub>2</sub> efflux rates of known magnitude from test surfaces. The laboratory evaluations confirmed the level of uncertainty derived from the many field comparisons, with differences sometimes exceeding a factor of two. An examination reported by Pumpanen et al. (2004), led them to conclude that “Any use of the static-chamber method ought to be particularly scrutinized.” Wang et al., (2004) compared results from closed and vented chambers, with results indicating differences in derived soil efflux rates (of ammonia [NH<sub>3</sub>] in their tests) ranging up to a factor of five.

Surface renewal approaches have been proposed to by-pass the obstacles associated with the physical presence of chambers (Paw U et al., 1995; Suvoarev et al., 2019). The incentive for such developments is the modification of the natural turbulence or stratification regime due to the chambers themselves. In the absence of a chamber, the layer of enriched air in contact with the out-gassing surface will display a concentration gradient depending on the circumstances and will slowly grow in depth. There are two principal considerations that arise. First, the presence of a chamber will disrupt the naturally occurring concentration gradient. Second, the air contained in the chamber will not reflect the characteristics of the external atmosphere. In the specific case of a stirred chamber, the air contained would likely be neutrally stratified, whereas the air outside it will be layered and stable. The radiometric properties (albedo and emissivity, in particular) of a chamber introduce additional concerns. Deriving results from chamber studies that relate to the situation when the chamber is absent presents sometimes confounding complexities. As yet, there is no method that appears to satisfy the objections of all critics.

Here, a statistical method is proposed, replicating the constraints associated with chamber methods in a way that leads to estimates of average fluxes rather than of specific short-term situations. The present intent is to demonstrate the utility of the methodology, without proposing that it should replace other experimental methods but indicating the benefits of an alternative, statistical way of looking at the results of field studies. The concept of a “virtual chamber” analysis to derive flux information from nighttime concentration data (of trace gases like NH<sub>3</sub>, CO<sub>2</sub>, methane [CH<sub>4</sub>], Rn, and the various nitrogen oxides [NO<sub>x</sub>]) arose in examination of data obtained in field studies of CO<sub>2</sub> and NH<sub>3</sub>. Both revealed the ramp structure at night considered to indicate trace gas accumulation in the stratified layers of air near the surface interrupted by nocturnal intermittent turbulence (Hicks et al., 2015).

### Core Ideas

- Statistical analysis reveals soil efflux rates at night.
- Analysis uses multiple regression to simulate closed or open chambers.
- Input data: rate of change of gas concentration, efficiency of vertical exchange, wind speed.
- The methodology minimizes the effects of limited fetch.
- Eddy-covariance measurements support CO<sub>2</sub> and NH<sub>3</sub> results.

## 2 | THEORY: THE VIRTUAL CHAMBER

Consider the case of trace gas emission from a specific surface. At this point, there is no consideration of the conventional requirement for time stationarity and spatial uniformity. These issues will be considered later. In daytime convective (and unstable) situations, the measurement of the fluxes is typically seen as a conventional micrometeorological exercise. At night, however, the constraints imposed by the necessary assumption that fluxes measured in the air at some convenient height above a surface of special interest are indeed representative of that particular surface presents substantial obstacles (Aubinet, 2008). It is the case of the nocturnal stratified atmosphere in contact with the surface that will be considered here.

There are many published examples of time series of measurements of trace gas concentration (e.g., CO<sub>2</sub> or CH<sub>4</sub>) in ground-level air that display a saw-tooth pattern at night, with slowly increasing concentrations interrupted by sharp decreases (e.g., Karipot et al., 2006). These intermittent decreases are commonly attributed to bursts of turbulence interrupting an otherwise quiescent surface boundary layer. There are several possible causes of these turbulent events, such as the oscillations of a low-level jet or the generation of gravity waves by some upwind obstacle (Aubinet, 2008). It is possible that the phenomena are a basic feature of strongly stratified flow (Manneville & Pomeau, 1979; He & Basu, 2015) as a consequence of interactions among different processes (Lorenz, 1963). The related phenomena are almost invariably external to the classical micrometeorological framework, in which turbulence is associated with the characteristics of the local surface. The optimal time resolution is therefore not associated with conventional micrometeorology, but instead short enough to identify with clarity occasions of intermittency so that these can be excluded from analysis intended to focus on the causes of increases in surface concentrations.

To illustrate the method now proposed, consider a field study in which a fast-response anemometer is deployed

at some convenient height ( $z_a$ ), providing vertical velocity variances every 5 min, or over some alternative averaging time deemed appropriate. In practice, use of a vertical propeller anemometer could suffice, but more often sonic anemometers are favored. Simultaneously, measurements of concentration ( $C$ ) of some atmospheric trace constituent are made, at some point ( $z_c$ ) below the anemometer installation. After data accumulation extending over many days, consider the statistical characteristics of ensembles of data generated after sorting according to time of day. A partial correlation examination of three variables is of present relevance:

$$X_1 = dC/dt \quad (1)$$

$$X_2 = u \quad (2)$$

$$X_3 = \sigma_w \quad (3)$$

where notation is conventional. In practice, the wind speed  $u$  is an output of the sonic anemometer, as is the standard deviation of the vertical wind component  $\sigma_w$ . The rate of change of concentration,  $dC/dt$ , is conveniently computed from the initial time sequence of measurement as:

$$dC/dt = (C_{n+1} - C_{n-1}) / (t_{n+1} - t_{n-1}) \quad (4)$$

where the measurement level of  $C$  ( $z_c$ ) is such that the lack of turbulence indicated by the sonic anemometer will also be indicative of a lack turbulent exchange at the height of measurement of  $C$ . A first-order partial correlation analysis (or multiple regression) yields the best-fitting coefficients in a relationship of the kind:

$$X_1 = a_x + b_{x12} \times X_2 + b_{x13} \times X_3 \quad (5)$$

The intercept  $a$  is therefore the value of  $X_1$  (i.e.,  $dC/dt$ ) that would be expected in the case for which  $X_2$  and  $X_3$  were both zero, that is, for when there is no effect of the wind (no advection) and no turbulent exchange in the vertical at the level of the anemometer ( $z_a$ ). The situation then envisioned is like that of a conventional closed chamber experiment, but lacking the consequences of a physical presence that could influence the natural circumstances.

In the event that measurements of  $\sigma_w$  are not available, any of several alternative measures are suitable as indicators of negligible turbulent exchange. For example, the classical Richardson number derived from gradient measurements of temperature and wind speed also satisfies the conceptual requirement. Bearing in mind that the approach outlined above specifies the wind speed as one of the major deter-

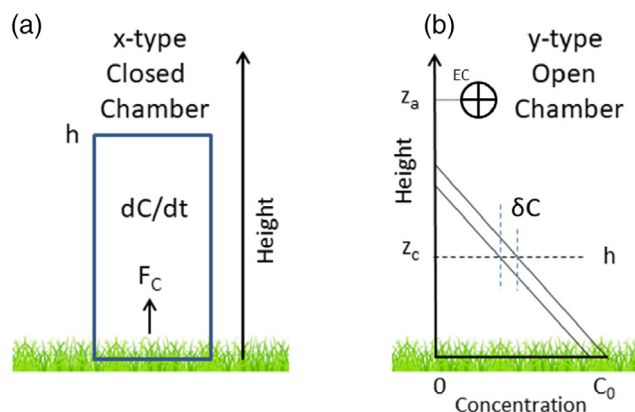


**FIGURE 1** Schematic illustrations of the concepts now being explored. The x-type chamber simulation is represented to the left, leading to an approximation that the efflux at the surface can be derived from measurements of the rate of change of concentration with time. An alternative y-type extreme is represented to the right, in which the depth of the layer of relevance is allowed to grow while maintaining the same concentration gradient. The height of measurement of  $\sigma_w$  by an eddy-covariance system (EC) is indicated as  $z_a$ .

mining properties, measurements of the temperature gradient alone would appear to suffice. However, in such cases where the desired extreme situation is quantified by a high numerical number (i.e.,  $Ri$  or  $dT/dz \rightarrow$  infinity) the statistical procedure retains its conceptual relevance only if the appropriate variable ( $X_3$ ) is derived as the inverse of these alternative properties. Hence  $Ri^{-1}$  or  $(dT/dz)^{-1}$  could be substituted for  $\sigma_w$  in constructing the variable  $X_3$ , without great loss of generality because the intent is to quantify the value of  $dC/dt$  when both  $X_2$  and  $X_3$  approach zero. For details of the relevant micrometeorology, see Garratt (1992).

Figure 1 presents a schematic illustration of the conceptual constructs now considered. Two configurations are illustrated. Consider, first, the closed-chamber option as discussed above and as illustrated in Figure 1a. In concept, the quantity  $C$  would best represent the average within the virtual chamber so defined, of cross-sectional area of  $1 \text{ m}^2$  and of height  $h$ . While this conceptual entity is defined in terms of specific measurable dimensions, its relevant characteristics are now based on the statistical extrapolation of other observations.

The model presented in Figure 1a is considered here to represent an extreme circumstance controlling the statistics that follow – a closed chamber. A second extreme is illustrated in Figure 1b, intended to represent an open chamber. In the latter case, the depth of the affected layer increases with time, according to the flux from the surface, but maintaining a constant gradient in the air. If the surface emission rate  $F_C$  is constant, then the total accumulation in the growing layer ( $\delta m$ ) will increase as the product  $\delta z \delta C$ . Since the change in height  $\delta z$  is proportional to  $\delta C$  (a linear dependence of  $C$  on

$z$  is assumed) and the efflux rate  $F_c$  is assumed constant, the increase of the mass of the constituent  $C$  must be proportional to  $(\delta C)^2$ . In the alternative closed chamber approximation, the change  $\delta m$  is proportional to  $\delta C$ , because the volume being filled is constant.

Hence, the virtual chamber can be considered in two ways, representing extremes. The first ( $x$  type) makes use of  $dC/dt$  as a key variable, with conceptual association with the operation of a closed but stirred chamber. The second ( $y$  type) is intended to simulate the characteristics of an open chamber, by substituting  $Y_1 = (dC/dt)^2$  for  $X_1 = dC/dt$  in the discussion above (specifically in Equation 1). In this second case, the eventual relationship sought is

$$Y_1 = a_y + b_{y12} \times X_2 + b_{y13} \times X_3 \quad (6)$$

which replicates Equation 5. The two separate estimates of the ensemble-mean average fluxes are then

$$F_x = h \times a_x \quad (7)$$

and

$$F_y = h \times a_y^{0.5} / 2 \quad (8)$$

where the divisor in Equation 8 arises from the consideration of a right-triangular conceptual configuration in the  $y$ -type case (as is evident in Figure 1b), rather than the rectangular figure that contains it in the  $x$  type (Figure 1a). The depth of relevance is assumed to be that of the concentration measurement, this assumed to simulate the top of the closed chamber in Figure 1a, and the depth for use in  $y$ -type calculations according to Figure 1b.

The discussion above relates to a situation in which  $\sigma_w$  data are routinely available. Such data are regularly provided by modern three-dimensional sonic anemometers, whose deployment is usually associated with the determination of fluxes by covariance between concentration and the vertical wind speed component, both measured at more than 1 Hz (typically 10 Hz). In the present case, the requirement that deployment must follow guidelines for accurate flux determination can be relaxed, because it is only the magnitude of  $\sigma_w$  that is needed. In Figure 1b the measurements of  $\sigma_w$  are assumed to be at a height ( $z_a$ ) above that of  $C$  measurement ( $z_c$ ). It is assumed that as  $\sigma_w$  trends to zero as stability increases at height  $z_a$ , so it does at a lower height  $z_c$ , or  $h$ .

The inclusion of wind speed is in recognition of the desire to eliminate advection as a major causative property, even though if the site in question is sufficiently uniform the wind speed contribution would be expected to become negligible. If fetch is limited and if the flux of interest can be associated solely with that fetch, then  $u x_f^{-1}$  becomes an attractive variable, where  $x_f$  is the upwind fetch.

The requisite analysis employs standard statistical methods, adapted from textbook examples (in which matrix algebra is commonly employed) for the present simple case by evaluating the correlation coefficients of relevance ( $R_{12}$  is the correlation coefficient between variables  $X_1$  and  $X_2$ ) and the resulting partial correlations ( $R_{12.3}$  is the partial correlation between variable  $X_1$  and  $X_2$  when the influence of variable  $X_3$  is accounted for). Of considerable relevance in analyses like that presented here are the consequent quantities

$$R_{1.23}^2 = R_{12.3}^2 (1 - R_{13}^2) + R_{13}^2 \quad (9)$$

$$R_{1.32}^2 = R_{31.2}^2 (1 - R_{12}^2) + R_{12}^2 \quad (10)$$

which enumerate the proportion of the variance in variable  $X_1$  that can be explained by the combination of variables  $X_2$  and  $X_3$ . Finding the equality evident in the two ways of deriving this quantity is a confidence-building exercise of some considerable satisfaction.

Standard statistical relationships lead immediately to the quantification of the variables  $a_x$  and  $a_y$  in Equations 5 and 6. Estimates of the effluxes then derive immediately, assuming that the height of measurement determines the average height used to define the conceptual chamber of relevance. This is a statistical matter that invites further examination.

In neither the closed-chamber or the open-chamber approximation can the results be considered actual measurements of the surface efflux rates. Rather, they are statistical estimates of these fluxes, based on the conceptual visualizations illustrated in Figure 1. In the following, two examples of recent application of the virtual chamber approach will be described. The first relates to a study of  $\text{CO}_2$  fluxes above an agricultural surface in central Ohio (O'Dell et al., 2018), making use of the Bowen ratio energy balance method (BREB) (q.v. Irmak et al., 2014). The second is based on a study of ammonia emissions from an area previously treated with urea ammonium nitrate (UAN) as a nitrogenous fertilizer, in central Illinois (Nelson et al., 2017, 2019). Both of these studies deployed a centrally located EC system. The EC data will be used here in comparison with results of the virtual chamber method. To maintain independence of the virtual chamber results from the EC data, the sonic anemometer quantifications of  $\sigma_w$  will not be used here as the variable  $X_3$  in the regressions. Temperature gradient measurements will be used instead, so that  $X_3$  will be taken to be  $\delta T^{-1}$ .

### 3 | THE OHIO $\text{CO}_2$ STUDY

Figure 2 shows the layout of the field site of the Ohio study of 2015 (O'Dell et al., 2018). Above each of two





**FIGURE 2** The surface layout of the test areas of the Ohio (2015) field study. White circles indicate the locations of Bowen ratio energy balance (BREB) measurement systems. The red circle shows where eddy-covariance measurements were made. The image is derived from Google Earth

test plots, measurements were made of the concentration of  $\text{CO}_2$  in air, the air temperature and vapor pressure at two levels close to the surface, wind speed, and the surface temperature as reported by downward looking infrared thermometers.

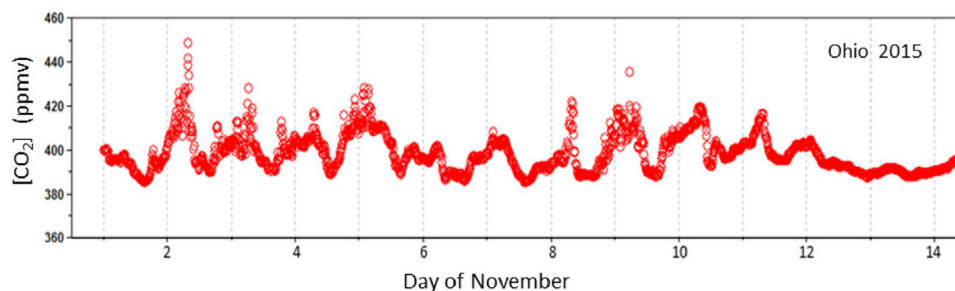
The two adjacent test areas (as seen in Figure 2), were each about 250 by 250 m in size. One of these test areas was tilled (Area 1), and the other not tilled (Area 2) before maize (*Zea mays* L.) was planted. Average values were recorded at 5-min intervals. A rotating arm system was used to measure differences in temperature and humidity between two heights. To eliminate the effects of sensor bias the resulting quantities were assembled into 10-min averages.

Figure 3 presents a sample time record of  $\text{CO}_2$  concentrations. The characteristic nighttime concentration build-ups are obvious, as are the consequences of intermittent turbulence. The Ohio site is within the mid-American farmlands and is subject to characteristic bursts of turbulence occurring at night (as have been investigated in detail by Banta, 2008, for example).

Midway between the two test areas an EC system was installed. This reported 5-min averages of the covariances,  $\overline{w'u'}$ ,  $\overline{w'T'}$ ,  $\overline{w'q'}$ , and  $\overline{w'C'}$ . It is the last of these that will serve as a reference for evaluation of the virtual chamber methods now discussed. On some occasions, the sonic anemometer yielded repeated highly improbable numbers and consequent non-physical quantifications of eddy fluxes. Causes of these periods of unusual values, usually occurring at night, have not been identified with certainty but are suspected to be associated with roosting birds. Such data have been rejected. After this data exclusion was implemented, some exceedances persisted. Following examination of the data streams, a simple data exclusion procedure was implemented. For every sequential data point, the average ( $\bar{x}$ ) and standard deviation  $\sigma_x$  of the preceding five measurements were calculated. Any data point outside the bounds  $\bar{x} \pm 4\sigma_x$  was identified as an outlier and was removed from consideration.

The selection of BREB data for use in the present illustration of the virtual chamber methodology has been based on the need to ensure independence from the sonic anemometer results to be used in comparison. Only nighttime data are considered. Hence, data records with reported positive net radiation have been excluded. Further, the intent is to interpret the increases in concentration observed near the surface in stable conditions. To this end, situations in which  $dC/d < 0$  have been rejected (since such situations are likely the consequence of nocturnal turbulence intermittency, another controlling mechanism to be considered elsewhere). To test the validity of the virtual chamber approach using BREB data alone, measurements of the virtual temperature gradient derived from the conventional BREB dataset have been used. To provide a measure of the limit as vertical mixing approaches zero  $X_2$  has been taken to be  $(\delta\theta_v)^{-1}$ , where  $\delta\theta_v$  is the virtual potential temperature difference between levels  $z_1$  and  $z_2$  (above the ground). In the present case,  $z_1$  was about 0.2 m and  $z_2$  about 1.8 m, so that the effective height to be used in the estimation of fluxes from the evaluations of  $a_x$  and  $a_y$  was about 1 m.

In Figure 4, an example is shown of the nighttime variation of the proportion of the variance in  $X_1$  and  $Y_1$  that can be accounted for by consideration of variables  $X_2$  and  $X_3$



**FIGURE 3** Time trends of  $\text{CO}_2$  concentration at a height of about 1 m above a recently harvested maize field in Ohio

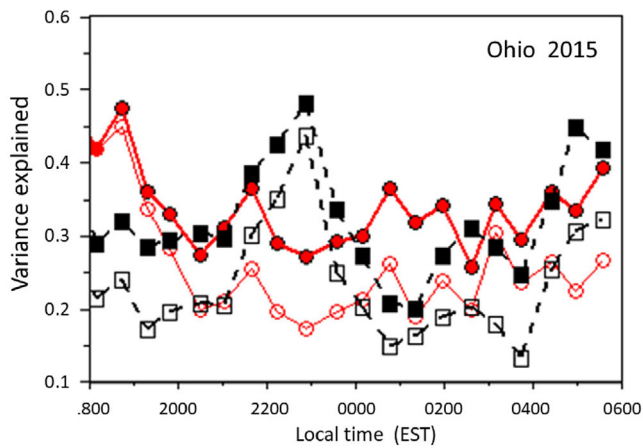


**FIGURE 4** The average variation during the night of the proportion of variance in  $dC/dt$  (closed chamber: solid symbols) and  $(dC/dt)^2$  (open chamber: open symbols) that can be accounted for by the present statistical treatment. Red circles relate to a previously-tilled area, black squares to an adjacent area not tilled

(following Equations 9 and 10). If this proportion is close to unity, then the data constitute a sound basis for examination in the way now suggested. However, such high values are not often encountered in the atmospheric surface boundary layer. For example, the relationship between the wind speed gradient and the surface stress is usually quantified by a correlation coefficient rarely exceeding 0.4, so that <20% of the variance in stress is accounted for by changes in components of the wind velocity. In this light, the values plotted in Figure 4 are somewhat reassuring, ranging from about 20–40%. It is noticeable, however, that the values associated with the open chamber ( $y$  type) assumption are lower than those of the closed chamber ( $x$  type). A low value of  $R_{x1.23}^2$  or  $R_{y1.23}^2$  is not a basis for disregarding the statistical results obtained but is certainly ground for considering them to be less robust. The data used in constructing Figure 4 are from October 2015, a period that included harvest and hence contained some unusual complexity. The illustration is selected to show a challenging example.

Figure 5 presents the estimates of surface effluxes derived from the present analysis. Three 2-wk periods are selected for presentation. Figure 5a is for the 2-wk period 16–29 June, shortly after emergence of the crop. Figure 5b is for 8–21 September (mature maize), and Figure 5c for 17–31 November (after harvest). These three examples are selected to show the range of results. The plots are of virtual chamber results derived from the closed chamber ( $x$  type, solid symbols) and open chamber ( $y$  type, open symbols) assumptions. As also in Figure 4, circles in red relate to Area 1 in Figure 2, previously tilled. Squares in black identify results for Area 2, not tilled. In green are shown the averages of EC results obtained during the same time frames, with fine lines identifying  $\pm 1$  SD bounds on the means. Inspection of

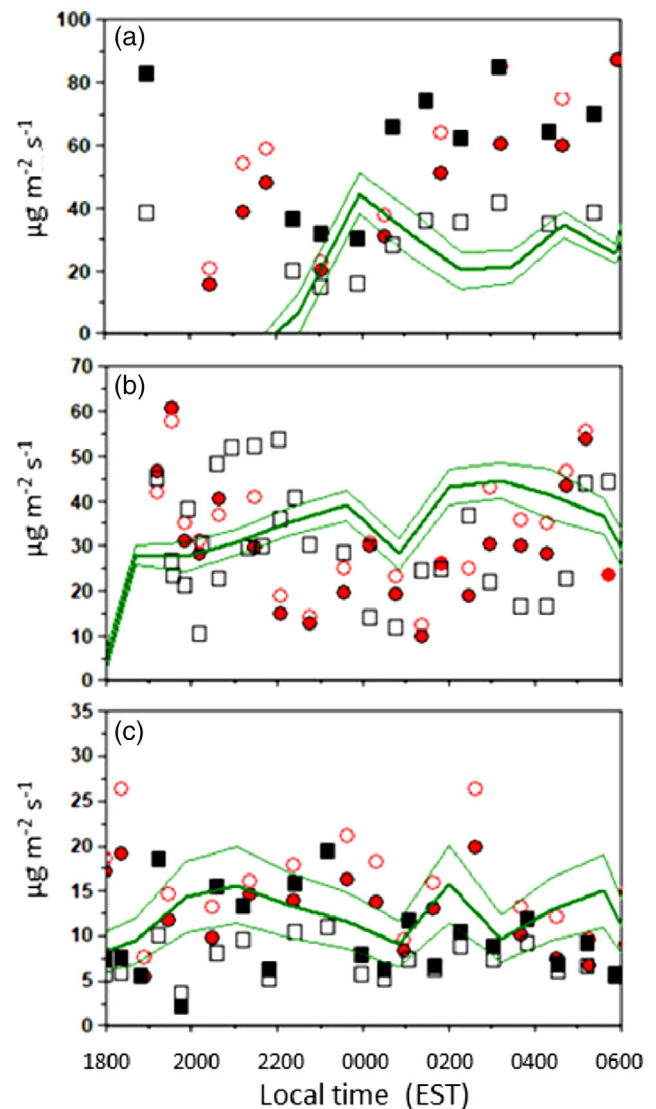


**FIGURE 5** From the Ohio  $\text{CO}_2$  study of 2015, three examples of results from virtual chamber and eddy-covariance methods: (a) for 16–29 June, (b) for 10–24 September, and (c) for 3–17 November. Solid symbols represent the closed chamber approach, open symbols the open chamber analogy. Red represents data from the northernmost plot (previously tilled), black from the untilled. The green line joins averages derived from eddy covariance; the fine green lines indicate the bounds corresponding to  $\pm 1$  SD on the mean

Figure 4 reveals that the  $x$ -type results generally exceed the  $y$  type. Moreover, fluxes from the previously tilled area (Area 1) exceed those from the untilled (Area 2). There being no obvious reason to prefer one of the two kinds of analysis rather than the other ( $x$  type vs.  $y$  type), it is presently preferred to accept both and to view them as extremes. In this case, a first-order conclusion would be to accept the geometric mean as the best estimate provided by the virtual chamber approach.



**FIGURE 6** As derived from Google Earth, a map of the 4-ha field site used in the Illinois (2014) study of ammonia fluxes following fertilization using urea ammonium nitrate

#### 4 | THE ILLINOIS $\text{NH}_3$ STUDY

Nelson et al. (2017) report a study of  $\text{NH}_3$  fluxes from an area previously fertilized with UAN. Such treatment is common in the midwestern United States. The site is illustrated in Figure 6. The volatilization of the ammonium delivered to the soil represents a loss of valuable nutrients from the soil and has been well studied. For example, Keller and Mengel (1986) report that a large part of the N delivered to the soil as UAN is subsequently lost from it by volatilization (in their study, about 30% was lost during the first 5 d after fertilization). Al-Kanani and McKenzie (1992) show that the rate of loss peaks soon after fertilization but drops markedly during the week that follows.

Like the Ohio site considered above, the Illinois location of present interest is located in the mid-American farmland region notorious for sporadic bursts of turbulence at night, attributed to many causes but often associated with the processes that lead to the development of nocturnal jets (q.v., Banta, 2008; Blackadar, 1957). The characteristic singularities in time traces of  $\text{NH}_3$  concentrations in air near the surface are evident in Figure 7, which shows a record of con-

centrations during a 1-wk part of the experimental period. It is assumed here that these irregular bursts of turbulence (regardless of their cause) curtail the otherwise steady accumulation of  $\text{NH}_3$  in the atmospheric boundary layer adjacent to the surface. The present intent is not to investigate these bursts of turbulence, but instead to accept them as features of the nighttime atmospheric environment (see Costa et al., 2011) and then to examine the trends with time when they are not contributing factors.

The primary intent of the Illinois study was to compare  $\text{NH}_3$  flux measurements derived using two methods: relaxed eddy accumulation (Businger & Oncley, 1990) and micrometeorological gradient analysis (Hicks & Wesely, 1978). Fertilization with UAN occurred on 6 May (Day 126) of 2014, and upward fluxes of  $\text{NH}_3$  peaked about 5 d later (Nelson et al., 2019). Soon after fertilization an EC system was installed, measuring  $\overline{w'u}$ ,  $\overline{w'T}$ , and  $\overline{w'q}$ . These fluxes were used in the subsequent micrometeorological analysis to quantify  $\text{NH}_3$  fluxes against which results from the presently proposed virtual chamber approach can be compared. Ammonia was measured using a cavity ring-down spectrometer (Picarro 2301).

The present analysis makes use of all available data with the same exclusions as were imposed on the Ohio  $\text{CO}_2$  dataset. Surviving data have been sorted according to time and assembled into sequential groups, each containing 25 “runs,” starting on Day 130. The virtual chamber results illustrated in Figure 8 are derived directly from these 25-member groupings. The paucity of data does not permit sequential consideration by time.

The  $\text{NH}_3$  concentrations are available only as 30-min averages. The virtual chamber techniques now proposed would work better with a finer time resolution, as was the case for the Ohio dataset considered above. The consequences of relying on a longer averaging time are apparent in Figure 8a, where the total proportion of variance explained in the rate of change of  $\text{NH}_3$  concentration with time is lower than was found for the Ohio  $\text{CO}_2$  data as shown in Figure 4. Nevertheless, the virtual chamber analysis appears to result in average effluxes much like those derived from the micrometeorological analysis, as is seen in Figure 8b.

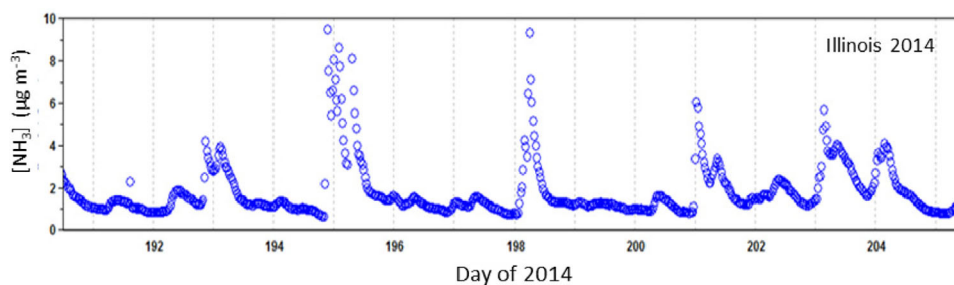


**FIGURE 7** A time sequence of  $\text{NH}_3$  concentration measurements obtained in the 2014 Illinois field study



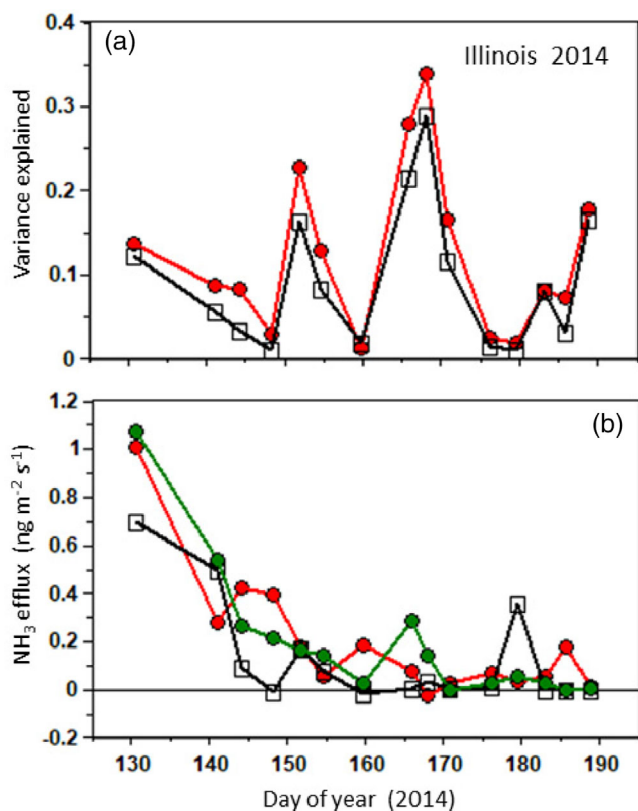


**FIGURE 8** Results derived from measurements of  $\text{NH}_3$  above a field previously fertilized with treatment of urea ammonium nitrate (UAN), in Illinois in 2014. Part (a) presents the total proportion of variance explained in  $dC/dt$  by the combined influences of wind speed and turbulent mixing, from interpretation of which (b) indicates how derived  $\text{NH}_3$  effluxes vary through the night. As before, (red) solid points indicate results obtained using the closed-chamber approximation described here, (black) open points represent vented chamber approximations. Average results from micrometeorological gradient analysis are plotted in green

The EC data were subject to periodic unexplained exceedances, presumably due to the roosting of birds or some other avian activity affecting the sonic anemometry and its associated high-frequency  $\text{NH}_3$  detector. To construct the averages plotted in Figure 8b, covariance data for each grouping have been rejected whenever a result exceeds the bounds corresponding to the average  $\pm 2$  SD. This process was repeated until no further application was required. The number of iterations was in the range 2–4.

Figure 8b provides an indication that the eventual rate of  $\text{NH}_3$  emission from the ground was about  $0.1 \text{ ng m}^{-2} \text{ s}^{-1}$ , having diminished rapidly from early values approaching  $1 \text{ ng m}^{-2} \text{ s}^{-1}$ . Wang et al. (2004) report that the rate of volatilization of  $\text{NH}_3$  from an area bearing a maize crop depends almost linearly on the amount of urea previously broadcast. The maximum  $\text{NH}_3$  emission rate is a few days following application of the fertilizer, at a rate of from  $0.1$  to  $0.8 \text{ kg ha}^{-1} \text{ d}^{-1}$ , corresponding to about  $100\text{--}800 \text{ } \mu\text{g m}^{-2} \text{ s}^{-1}$ .

The first efflux estimate derived from the present analysis is about three orders of magnitude lower. In all comparisons of this kind, it should be remembered that classical chamber study results are typically presented as whole-day averages, whereas the virtual chamber results now being considered represent only those times of the day when the air in contact with the surface is stratified, usually at night. Once again, the difference invites investigation.

## 5 | DISCUSSION AND CONCLUSIONS

In the current environment of stressed ecosystems and climate change, the emissions of trace gases from soils can be important. For example, climate change models require an accurate depiction of the generation rate of  $\text{CO}_2$  by terrestrial subsurface microbial activity. In similar vein, assessments of the role of  $\text{CH}_4$  in the context of climate change modeling also require an understanding of the roles of such potential sources as anaerobic saltwater swamps and permafrost. In many experimental programs, BREB methods and a variety of other micrometeorological approaches are used, but for several reasons these are poorly appropriate at night. The experimental areas involved are typically small; such that they violate the fetch and time stationarity requirements of standard micrometeorology. Moreover, the analysis assumes a strong relationship between fluxes and gradients that appears unlikely in conditions of stable stratification and is weak at the best of times. At night, the fluxes can result from intermittent periods of turbulence interspaced with long periods of quiescence. Any assumption that the fluxes measured over any particular nighttime period relate to gradients measured at the same time seems courageous.

The variety of methods currently used to quantify soil efflux rates has generated many comparison experiments (e.g., Norman et al., 1997) but debate continues about which of the alternatives would be most appropriate for a particular experimental situation (Brændholt, Larsen, Ibrom, & Pilegaard, 2017). The methodology presented here diverges substantially from such familiar experimental strategies. First, it is focused on the ground itself (or the vegetation above it) and does not rely on the assumption that measurements made above the ground are indicative of the local surface. Second, the use of statistical methods to drive the analysis towards situations in which the prevailing stability is high but the wind speed is zero reduces (if not eliminates) the conventional requirement regarding large fetches. In this regard, the extrapolation of observations on which the analysis relies equates to an immunization from strong fetch effects. Third, the method requires measurement with a time resolution such that intermittent bursts of turbulence can be identified and eliminated. This is in direct contrast to standard micrometeorological practice, which requires a sampling duration long



enough that a statistically significant sampling of these same bursts of turbulence can be obtained.

Field experience indicates that a time resolution of the trace gas concentration record should best be such that events shorter than 5 min can be resolved, but the availability of such data is currently limiting. Reliance on data that fail to permit fine distinction between periods of turbulence bursting and the quiescent periods between successive intermittent burst occurrences certainly obscures the statistical correlations on which the present techniques are based, and will result in an underestimation of the efflux in question.

The present intent has been to make use of two different datasets to illustrate the potential utility of the virtual chamber analytical methodology and not to focus on results from any specific location in detail. Such exploration is left to others who are sufficiently enthused to explore the matter further. However, it is clear the  $\text{NH}_3$  data derived from the virtual chamber approach yield averages of the same order as EC measurements, and that the Ohio  $\text{CO}_2$  dataset yields similar results.

The methods now presented do not result in a more than a statistical estimate of soil effluxes. It is assumed that the two alternative methods discussed here represent extremes, so that the exchange rates of actual relevance lie between the corresponding bounds. A similar line of thinking was proposed by Wang et al. (2004), whose results derived from field studies over the North China Plain using both closed and vented chambers. These two experimental methods yielded flux estimates that differed by as much as an order of magnitude. Hence, the small differences found in the studies now considered appear reasonable, although requiring additional research.

It is thought that the methodologies presented here will be found most useful in extraction of meaningful soil flux estimates in continuing strongly stable conditions, such as are often encountered over land at night and over wetlands and lakes in daytime. Additional tests of the virtual chamber technique are planned, with increased attention to comparisons involving the interpretation of trace gas concentrations obtained with fine time resolution (~1 min) and exchange rates yielded by other methods (such as EC 15-min averages).

## ACKNOWLEDGMENTS

The Illinois  $\text{NH}_3$  study was funded by the National Science Foundation (Award nos. AGS12-36814 and AGS 12-33458). The Ohio  $\text{CO}_2$  study was a component of the research program of the University of Tennessee. Suggestions from a reviewer (TF) have served to improve the current presentation greatly. The scientific results and conclusions, as well as any views or opinions expressed herein, are those of the authors and do not necessarily reflect the views of any of the sponsors.

## CONFLICT OF INTEREST

The present authors have no conflicts regarding the conduct of this work or its presentation.

## AUTHOR CONTRIBUTIONS

B.B. Hicks: Conceptualization; Formal analysis; Methodology; Project administration; Software; Supervision; Writing-original draft; Writing-review & editing. N. Lichiheb: Data curation; Investigation; Methodology; Software; Validation; Writing-review & editing. D.L. O'Dell: Data curation; Formal analysis; Investigation; Methodology; Project administration; Validation; Writing-review & editing. J.N. Oetting: Conceptualization; Formal analysis; Methodology; Writing-review & editing. N.S. Eash: Data curation; Funding acquisition; Investigation; Project administration; Resources; Supervision; Writing-review & editing. M. Heuer: Data curation; Investigation; Methodology; Validation; Writing-review & editing. Latoya Myles: Data curation; Funding acquisition; Investigation; Methodology; Project administration; Resources; Supervision. L. Myles: Data curation; Funding acquisition; Investigation; Methodology; Project administration; Resources; Supervision.

## ORCID

Bruce B. Hicks  <https://orcid.org/0000-0002-0989-9310>

Deb. L. O'Dell  <https://orcid.org/0000-0003-4968-2287>

## REFERENCES

- Al-Kanani, T., & MacKenzie, A. J. (1992). Effect of tillage practices and hay straw on ammonia volatilization from nitrogen fertilizer solutions. *Canadian Journal of Soil Science*, 72, 145–157. <https://doi.org/10.4141/cjss92-014>
- Aubinet, M. (2008). Eddy covariance  $\text{CO}_2$  flux measurements in nocturnal conditions: An analysis of the problem. *Ecological Applications*, 18, 1368–1378. <https://doi.org/10.1890/06-1336.1>
- Banta, R. M. (2008). Stable-boundary-layer regimes from the perspective of the low-level jet. *Acta Geophysica*, 56, 58–87. <https://doi.org/10.2478/s11600-007-0049-8>
- Blackadar, A. K. (1957). Boundary layer wind maxima and their significance for the growth of nocturnal inversions. *Bulletin of the American Meteorological Society*, 38, 283–290. <https://doi.org/10.1175/1520-0477-38.5.283>
- Brændholt, A., Larsen, K. S., Ibrom, A., & Pilegaard, K. (2017). Overestimation of closed-chamber soil  $\text{CO}_2$  effluxes at low atmospheric turbulence. *Biogeoscience*, 14, 1603–1616. <https://doi.org/10.5194/bg-14-1603-2017>
- Businger, J. A., & Oncley, S. P. (1990). Flux measurement with conditional sampling. *Journal of Atmospheric and Oceanic Technology*, 7, 349–352. [https://doi.org/10.1175/1520-0426\(1990\)007%3c0349:FMWCS%3e2.0.CO;2](https://doi.org/10.1175/1520-0426(1990)007%3c0349:FMWCS%3e2.0.CO;2)
- Darenova, E., Pavelka, M., & Acosta, M. (2014). Diurnal deviations in the relationship between  $\text{CO}_2$  efflux and temperature: A case study. *Catena*, 123, 263–269. <https://doi.org/10.1016/j.catena.2014.08.008>
- Edwards, N. T. (1982). The use of soda-lime for measuring respiration rates in terrestrial systems. *Pedobiologia*, 23, 321–330.

- Garratt, J. R. (1992). *The atmospheric boundary layer*. Cambridge: Cambridge University Press.
- He, P., & Basu, S. (2015). Direct numerical simulation of intermittent turbulence under stably stratified conditions. *Nonlinear Processes Geophysics*, 22, 447–441. <https://doi.org/10.5194/npg-22-447-2015>
- Hicks, B. B., O'Dell, D. L., Eash, N. S., & Sauer, T. (2015). Nocturnal intermittency in surface CO<sub>2</sub> concentrations in Sub-Saharan Africa. *Agricultural and Forest Meteorology*, 25, 129–134. <https://doi.org/10.1016/j.agrformet.2014.09.007>
- Hicks, B. B., & Wesely, M. L. (1978). An examination of some micrometeorological methods for measuring dry deposition (Report EPA-600/7-78-116). Washington, DC: U.S. Environmental Protection Agency.
- Irmak, S., Skaggs, K. E., & Chatterjee, S. (2014). A review of the Bowen ratio surface energy balance method for quantifying evapotranspiration and other energy fluxes. *Transactions of the ASABE*, 57, 1657–1674.
- Karipot, A., Leclerc, M. Y., Zhang, G., Martin, T., Starr, G., Hollinger, D., ... Hendrey, G. R. (2006). Nocturnal CO<sub>2</sub> exchange over a tall forest canopy associated with intermittent low-level jet activity. *Theoretical and Applied Climatology*, 85, 243–248. <https://doi.org/10.1007/s00704-005-0183-7>
- Keller, G. D., & Mengel, D. B. (1986). Ammonia volatilization from nitrogen fertilizers surface applied to no-till corn. *Soil Science Society of America Journal*, 50, 1060–1063. <https://doi.org/10.2136/sssaj1986.03615995005000040045x>
- Lorenz, E. N. (1963). Deterministic nonperiodic flow. *Journal of Atmospheric Science*, 20, 130–141. [https://doi.org/10.1175/1520-0469\(1963\)020%3c0130:DNF%3e2.0.CO;2](https://doi.org/10.1175/1520-0469(1963)020%3c0130:DNF%3e2.0.CO;2)
- Meyers, T. P., Hall, M. E., Lindberg, S. E., & Kim, K. I. (1996). Use of the modified Bowen-ratio technique to measure fluxes of trace gases. *Atmospheric Environment*, 30, 3321–3329. [https://doi.org/10.1016/1352-2310\(96\)00082-9](https://doi.org/10.1016/1352-2310(96)00082-9)
- Nay, S. M., Mattson, K. G., & Bormann, B. T. (1994). Biases of chamber methods for measuring soil CO<sub>2</sub> efflux demonstrated with a laboratory apparatus. *Ecology*, 75, 2460–2463. <https://doi.org/10.2307/1940900>
- Nelson, A. J., Koloutsou-Vakakis, S., Rood, M. J., Myles, L., Lehmann, C., Bernacchi, C., Balasubramanian, S., Joo, E., Heuer, M., Vieira-Filho, M., & Lin, J. (2017). Season-long ammonia flux measurements above fertilized corn in central Illinois, USA, using relaxed eddy accumulation. *Agricultural and Forest Meteorology*, 239, 202–212. <https://doi.org/10.1016/j.agrformet.2017.03.010>
- Nelson, A. J., Lichiheb, N., Koloutsou-Vakakis, S., Rood, M. J., Heuer, M., Myles, L., Joo, E., Miller, J., & Bernacchi, C. (2019). Ammonia flux measurements above a corn canopy using relaxed eddy accumulation and a flux gradient system. *Agricultural and Forest Meteorology*, 264, 104–113. <https://doi.org/10.1016/j.agrformet.2018.10.003>
- Norman, J. M., Garcia, R., & Verma, S. B. (1992). Soil surface CO<sub>2</sub> fluxes and the carbon budget of grassland. *Journal of Geophysical Research*, 97(D17), 18,845–18,853. <https://doi.org/10.1029/92JD01348>
- Norman, J. M., Kucharik, C. J., Gower, S. T., Baldocchi, D. D., Crill, P. M., Rayment, M., Savage, K., & Striegl, R. G. (1997). A comparison of six methods for measuring soil-surface carbon dioxide fluxes. *Journal of Geophysical Research*, 102(D24), 28,771–28,777. <https://doi.org/10.1029/97JD01440>
- O'Dell, D. L., Eash, N. S., Hicks, B. B., Oetting, J. N., Sauer, T. J., Lambert, D. M., ... Zahn, J. A. (2018). Reducing CO<sub>2</sub> flux by decreasing tillage in Ohio: Overcoming conjecture with data. *Journal of Agricultural Science*, 7, 1–15.
- Paw U, K. T., Qiu, J., Su, H.-B., Watanabe, T., & Brunet, Y. (1995). Surface renewal analysis: A new method to obtain scalar fluxes. *Agricultural and Forest Meteorology*, 74, 119–137. [https://doi.org/10.1016/0168-1923\(94\)02182-J](https://doi.org/10.1016/0168-1923(94)02182-J)
- Pumpanen, J., Kolari, P., Ilvesniemi, H., Minkinen, K., Vesala, T., Niinistö, S., Lohila, A., Larmola, T., Morero, M., Pihlatie, M., Janssens, I., Yuste, J. C., Grünzweig, J. M., Reth, S., Subke, J.-A., Savage, K., Kutsch, W., Østreg, G., Ziegler, W., ... Hari, P. (2004). Comparison of different chamber techniques for measuring soil CO<sub>2</sub> efflux. *Agricultural and Forest Meteorology*, 123, 159–176. <https://doi.org/10.1016/j.agrformet.2003.12.001>
- Schneider, J., Kutzbach, L., Schulz, S., & Wilmking, M. (2009). Overestimation of CO<sub>2</sub> respiration fluxes by the closed chamber method in low-turbulence nighttime conditions. *Journal of Geophysical Research-Biogeosciences*, 114, G03005. <https://doi.org/10.1029/2008JG000909>
- Skiba, U., Drewer, J., Tang, Y. S., van Dijk, N., Helfter, C., Nemitz, E., ... Sutton, M. A. (2009). Biosphere-atmosphere exchange of reactive nitrogen and greenhouse gases at the NitroEurope core flux measurement sites: Measurement strategy and first data sets. *Agriculture, Ecosystems & Environment*, 133, 139–149.
- Suvočarev, K., Castellvi, F., Reba, M. L., & Runkle, B. R. K. (2019). Surface renewal measurements of H<sub>2</sub>O and CO<sub>2</sub> fluxes over two different agricultural systems. *Agricultural and Forest Meteorology*, 279, 107763. <https://doi.org/10.1016/j.agrformet.2019.107763>
- Wang, Z.-H., Liu, X.-J., Ju, X.-T., Zhang, F.-S., & Malhi, S. S. (2004). Ammonia volatilization loss from surface-broadcast urea: Comparison of vented- and closed-chamber methods and loss in winter wheat-summer maize rotation in North China Plain. *Communications in Soil Science and Plant Analysis*, 35, 2,917–2,939. <https://doi.org/10.1081/CSS-200036499>
- Wilson, T. B., Meyers, T. P., Kochendorfer, J., Anderson, M. C., & Heuer, M. (2012). The effect of soil surface litter residue on energy and carbon fluxes in a deciduous forest. *Agricultural and Forest Meteorology*, 161, 134–147. <https://doi.org/10.1016/j.agrformet.2012.03.013>

**How to cite this article:** Hicks BB, Lichiheb N, O'Dell DL, et al. A statistical approach to surface renewal: The virtual chamber concept. *Agrosyst Geosci Environ*. 2021;4:e20141. <https://doi.org/10.1002/agg2.20141>